

Contents lists available at ScienceDirect

# Geoderma

journal homepage: www.elsevier.com/locate/geoderma





# Chemical and hydrological controls on salt accumulation in irrigated soils of southwestern U.S

Anna C. Ortiz\*, Lixin Jin

The Department of Geological Sciences, The University of Texas at El Paso, 500 W. University Ave., El Paso, TX 79968, United States

#### ARTICLE INFO

Handling Editor: Morgan Cristine L.S.

Keywords:
Aridland agriculture
Soil texture
Flood irrigation
Salt accumulation
Sodium adsorption ratio (SAR)

#### ABSTRACT

Soil salinization is a global problem affecting approximately 10% of agricultural soils, particularly in irrigated aridlands. This study quantified salt-loading by flood irrigation and soil fertilizers/amendments versus atmospheric deposition, studied controls of solute transport and salt buildup, and evaluated the effectiveness of gypsum application in improving soil sodicity in the arid southwestern United States. Study sites include one natural site and two agricultural sites in fields of dominant crops of the region, a pecan orchard and an alfalfa field near El Paso, Texas. The salt-loading rate in agricultural soils was dominated by the quantity and quality of irrigation waters rather than by dust. Salt loadings by irrigation waters were estimated  $\sim 306$  g Na $^+$  m $^{-2}$  yr $^{-1}$  $129 \text{ g Ca}^{2+} \text{ m}^{-2} \text{ yr}^{-1}$ , 361 g Cl $^{-}$  m $^{-2}$  yr $^{-1}$ , 419 g SO $_4^{2-}$  m $^{-2}$  yr $^{-1}$ , and 284 g HCO $_3^{-}$  m $^{-2}$  yr $^{-1}$ , followed by soil amendments. Whereas dust and fertilizer loadings were negligible in agricultural soils. Soil texture variability physically governs water movement and solute transport; coarser soils retained significantly less water than finer soils upon irrigation (p < 0.005) facilitating salt leaching. More salts accumulated around low-permeability layers. Some soils have approached salinity thresholds after only 90 years of cultivation. The Rio Grande river flow is projected to decrease due to reduced snowfall in Colorado, leading to more groundwater of higher salinity, to be used. If ground water were to be the sole water source, the salt loading rate would almost double. Soil amendments temporarily reduce soil sodicity induced by high Na<sup>+</sup> concentrations in irrigation water. Their application is needed annually to prevent soil dispersion, to improve infiltration, and to stop even faster salt accumulation. This study highlighted the challenges that the Rio Grande valley in southwestern United States and other irrigated drylands are facing.

# 1. Opportunities and challenges of irrigated agriculture in aridlands: Rio Grande valley

More than 40% of the Earth's land are covered as aridlands; they are characterized by relatively low precipitation and high potential evapotranspiration, expressed in long periods of water deficiency and lower biomass (e.g., Grace et al., 2006; Reynolds et al., 2007; Wang et al., 2012). A large portion of natural aridlands have been converted to cultivated fields while still providing a home to more than 38% of the world's population (Crutzen, 2002; Reynolds et al., 2007). Irrigation increases crop yield potential substantially, when compared to rain-fed agriculture (Kukal and Irmak, 2019).

When freshwater resources are limited (Rozema and Flowers, 2008; Assouline et al., 2015), surface and groundwaters waters, high in salinity, are used for irrigation. Evaporative water loss, limited water infiltration, and irrigation water of high salinity lead to the

accumulation of evaporite salts near impermeable soil horizons. These secondary salts clog soil pores, decreasing salt leaching, facilitating future evaporation and accelerating future salt buildup (e.g., Assouline et al., 2015; Cox et al., 2018). Soil salinization from irrigated agriculture has been recorded worldwide, including in countries like the United States, Argentina, Zimbabwe and China (e.g., Falasca et al., 2014; Shrivastava and Kumar, 2015; Chemura et al., 2014; Wang et al., 2015), and it has been responsible for lowering crop yields and deteriorating overall soil quality (Pannell and Ewing, 2006; Shrivastava and Kumar, 2015; Cox et al., 2018). Altogether, soil salinization affects more than 830 million ha of land globally, or 8.3 million km², or ~10% of the world's arable land (Szablocs, 1989; Martinez-Beltran and Manzur, 2005). The lack of irrigation water and soil salinity problems have been estimated to lead to multibillion-dollar losses in crop cultivation in arid environments (Qadir et al., 2014).

Soil salinity can be measured as electrical conductivity (EC) or as

<sup>\*</sup> Corresponding author at: Williams Hall, 101 Derieux Pl, Raleigh, NC 27607, United States. *E-mail addresses*: anna.ortiz@usda.gov (A.C. Ortiz), ljin2@utep.edu (L. Jin).

total dissolved solids (TDS) in soil pastes or as osmotic potential (Brandy and Weil, 2008). A soil is considered saline when EC values are greater than 4 dS m<sup>-1</sup>, approximately equivalent to 40 mM of NaCl (Marschner, 1995). Sodicity is another measure of soil quality that can control clay behavior, soil structure and soil permeability (Richards, 1954; Brandy and Weil, 2008). The sodium adsorption ratio (SAR) is a widely used proxy of soil sodicity, similar to the cation ratio of structural stability (CROSS) that can be used to assess irrigation water and soil leachate's sodicity (Rengasamy and Marchuk 2011). Briefly, SAR is the ratio of sodium concentration over the square root of the sum of calcium and magnesium concentrations in a soil slurry. Soils are considered sodic if SAR values are greater than 13 (Essington, 2003; Chaganti and Crohn, 2015). Under sodic conditions, clay disperses, greatly decreasing soil permeability and hydraulic conductivity (Assouline et al., 2015; Qi et al., 2018). Soils that are both sodic and saline are treated for sodicity first because sodic conditions lead to increased clay dispersion, limiting water movement and increasing the amount of salt accumulation (Lal et al., 1989).

The Rio Grande is the fifth longest river in the United States, approximately 80% of its annual flow is diverted for municipal and agricultural, serving over 5 million people along its course (Woodhouse et al., 2005; Hall and Peterson, 2013). Due to both natural processes and human activities, including agriculture, the salinity of the Rio Grande increases downstream (Hogan et al., 2007; Williams et al., 2013; Szynkiewicz et al., 2015). For example, the EC values of the Rio Grande water near the El Paso, TX region, were measured at  $\sim\!1.4\!-\!4.6$  dS m $^{-1}$  in 2009–2010, near saturation or slightly oversaturated for calcite (CaCO3), unsaturated for gypsum (CaSO4\*2H2O) and halite (NaCl) (Szynkiewicz et al., 2015). Moreover, decreased snowfall at its headwaters in Colorado, is projected to reduce the Rio Grande river's water flow (Chavarria and Gutzler, 2018; Elias et al., 2015; Pascolini-Campbell et al., 2017).

Large portions of land along the mid-Rio Grande are used for cultivation, with three major agricultural hotspots: Albuquerque (New Mexico, USA), Las Cruces (New Mexico, USA) and El Paso (Texas, USA). Typically, fields are flooded with several centimeters of Rio Grande water per irrigation event, a common and low infrastructure practice. Irrigated agriculture in El Paso supports major crops such as alfalfa (Medicago sativa), cotton (Gossypium barbadense) and pecan (Carya illinoinensis), which have relatively high salt tolerances (2 dS m<sup>-1</sup>,~7 dS  $m^{-1}$ , and  $\sim 3 dS m^{-1}$ ) (Mass and Hoffman, 1977; Miyamoto et al, 1986). In 2012, 25.4% of land use in the El Paso County, Texas, was registered as cropland and was second in pecan production in the State of Texas (USDA-NASS). Occurrence of drought in the headwaters and tributaries affects the total supply of the Rio Grande water accessible to Texan farmers (International Boundary & Water Commission). During drought, when river water is not sufficient during a growing season, groundwater or treated municipal wastewater is used for irrigation in pecan orchards. Alfalfa fields; however, are typically fallowed in years of drought.

Aeolian dust is prevalent in aridlands, and has long been recognized as the predominant Ca source in the formation of natural pedogenic carbonate in the American Southwest (e.g. Gile, 1961; Chiquet et al., 1999, 2000; Capo and Chadwick, 1999; Naiman et al., 2000). Although atmospheric deposition, high evapotranspiration and salt accumulation are naturally occurring, it is important to determine if secondary salt formation is enhanced by agricultural management practices, outpacing the natural processes.

Cox et al. (2018) collected 60-cm soil profiles from three major regional crops (cotton, alfalfa, and pecan) along the Rio Grande valley and reported high soil sodicity and salinity as a result of 90 years of cultivation with flood irrigation. Soil texture was identified to strongly impact water flow paths, residence time and to control the magnitude and location of salt accumulation (Cox et al., 2018). Growers actively combat limited water availability, soil salinization and sodicity with management practices including leaving crops like alfalfa fallow, physical and chemical strategies like deep plowing, irrigating fields with

excess waters, and additions of gypsum, sulfuric acid, or elemental sulfur onto problem areas (Ganjegunte et al., 2018). Plowing, resurfaces deeper soils of lower salinity, facilitating water infiltration. Irrigating fields before the growing season can flush pre-existing secondary salts to prepare soils for the growing season. Chemicals such as gypsum, sulfuric acid and sulfur pellets are used to lower sodicity and maximize the effects of salt leaching. Briefly, calcium dissolved from gypsum replaces sodium that is adsorbed in clays, allowing clay aggregation, improving permeability, and enabling sodium loss during leaching. Sulfuric acid, either applied directly or formed from oxidation of elemental sulfur pellets, dissolves soil carbonates and produces gypsum. This practice not only lowers the sodicity, but also lowers the pH, and increases soil porosity by congruent dissolution of existing carbonates.

This study builds on previous work to: (1) quantify atmospheric (i.e., wet and dry deposition) versus anthropogenic (agricultural amendments and flood irrigation) salt inputs to local agricultural soils, (2) investigate the importance of different controls on salt accumulation rates and (3) determine if soil amendments improve long-term soil quality.

#### 2. Methods

#### 2.1. Site description

Historic flooding and meandering of the Rio Grande river have deposited a variety of inter-fingerings of sand, silt and clay particles of Holocene-age (Doser et al., 2007, 2019). Soils that are developed on these sediments are typically alkaline Entisols, with no discernable horizons (Miyamoto, 2010). Two agricultural study sites were selected along the Rio Grande valley from an alfalfa field and a pecan orchard, covering typical crops of the region (Fig. 1), the same alfalfa and pecan orchards as in Cox et al. (2018).

The pecan orchard in Tornillo, Texas, USA had previously grown cotton for 50 years prior to changing to pecan for the last 30 years. During growing season (April-October), the pecan field is flooded with approximately 10 cm of irrigation water every 2 to 3 weeks, about 1.5 m of water per growing season. At the pecan orchard, irrigation waters are primarily from the Rio Grande, and supplemented with local ground water from two wells. These wells were drilled to depths of 36 and 62 m, respectively, accessing water in Rio Grande alluvium system.

Fertilizers, liquid or easily soluble salts, including potassium carbonate, urea, and humic acids are applied annually to improve crop yields and solid amendments are applied to improve soil quality (Appendix Table 1A). For example,  $56~{\rm g~m^{-2}}$  of elemental sulfur pellets have been applied annually to lower soil sodicity for the past 20 years. Gypsum is added periodically and selectively to areas with severe sodicity, and the average application rate is estimated at  $125-250~{\rm g~m^{-2}}$  yr $^{-1}$ . Soils are typically tilled to  $15~{\rm cm}$  every spring to mix fertilizers and amendments well. Soils in the pecan orchard belong to the Saneli siltyclay loam, Harkey loam, and Tigua silty-clay series (NRCS).

The alfalfa field is in southeastern El Paso, Texas and soils there are Harkey silty clay loam series (NRCS). In contrast to the pecan site, the alfalfa site has not been fertilized, amended, or tilled. Ground waters have never been used for irrigation at the alfalfa site; fields are left fallow if Rio Grande waters are insufficient.

A natural site was selected in the outskirts of Fabens, Texas, with no current or historically documented agricultural land use (Fig. 1). Dominant soils at the natural site are wind-modified sandy alluvium from the Bluepoint association with surrounding soils of Pleistocene-age (NRSC Custom Soil Report). The natural site is characterized by Chihuahuan Desert scrub, dominated by mesquite (*Prosopis glandulosa*) and creosote bush (*Larrea tridentata*) among bare lands of aeolian deposits and a few sand-dune mounds.

# 2.2. Solid sample collection: dust, soils, and soil amendments

Dust samples were collected with passive dust-pans in both the pecan

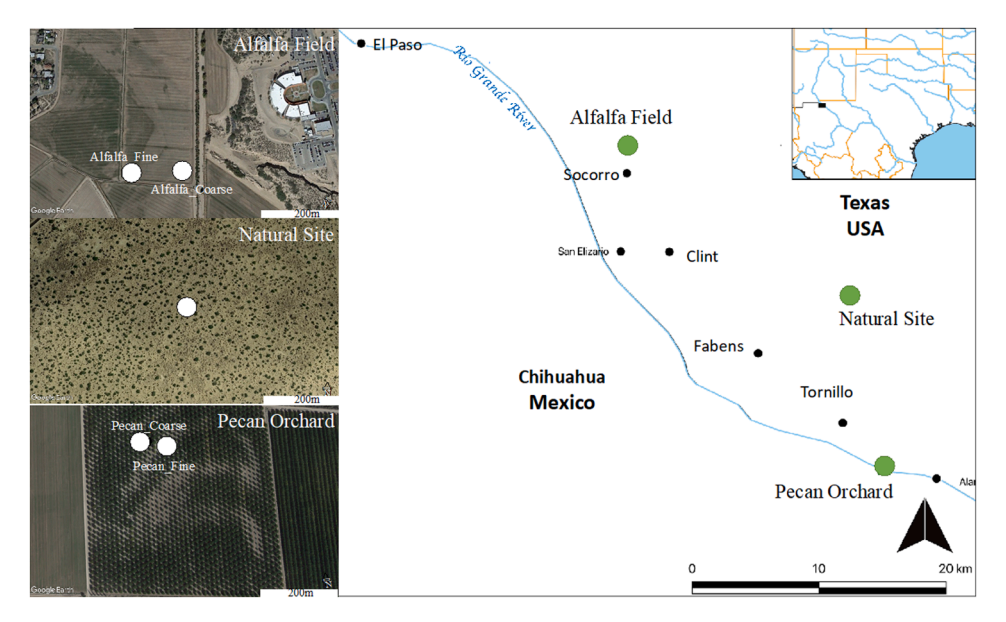


Fig. 1. Regional Map of three study sites in the El Paso, TX region, along the Rio Grande valley: two agricultural sites Alfalfa and Pecan and one natural site near Fabens. In both agricultural sites, two soil profiles were chosen: Pecan\_Fine and Pecan\_Coarse, and Alfalfa\_Fine and Alfalfa\_Coarse. Arial photographs are shown to highlight vegetation differences within a field.

and natural sites for exactly one year, following the methods in Ganor (1975) and Shannak et al. (2014). Specifically, an aluminum pan filled with glass beads was attached to a vertical pole that was  $1.5\,\mathrm{m}$  above the ground surface. After one year, the sample from each pan was weighed, then the flux was calculated using the weight, the dimension of the dust-pan ( $0.14\,\mathrm{m}^2$ ) and the duration of the dust deposition (one year). Presumably, a dust-pan sample contains both wet and dry deposition and represents annual atmospheric deposition. Elemental analyses of dust samples are discussed below along with soils.

At the pecan orchard, two soil profiles were collected, one near visually stunted pecan tree growth (referred to as Pecan\_Fine) and the other near visually lush growth (referred to as Pecan\_Coarse) (Fig. 1). Soil samples were collected with a manual soil auger in 10 cm intervals until 300 cm below the surface, which was the depth of the water table at the time of sampling. A drainage canal runs along the northern edge of the pecan orchard,  $\sim\!150$  m from the Pecan\_Coarse and Pecan\_Fine sites, with water level approximately 4 m below the ground surface during the irrigation season.

An additional soil profile (Pecan\_AG) was collected near Pecan\_Fine, also near Pecan1 in Cox et al. (2018), right after gypsum application. This was to compare with soil data from Cox et al. (2018) before gypsum application (Pecan\_BG) and determine the impact of amendments on soil sodicity. Pecan\_AG and Pecan\_BG profiles reached 70 and 80 cm, respectively with 10 cm resolution.

During a fallow year, two soil profiles were also collected near visually lush and stunted alfalfa (Alfalfa\_Fine and Alfalfa\_Coarse, respectively; Fig. 1) (Cox et al., 2018; Doser et al., 2019). Soils were augured in February 2013 with 10 or 20 cm resolution, from 0 to 300 cm below land surface. A 60-cm soil profile was previously collected next to Alfalfa\_Fine as "Alfalfa" by Cox et al. (2018), and relabeled as Alfalfa\_Fine\_D, as a shallow duplicate. These soil samples were analyzed for more chemical data.

Soil samples at  $\sim 10$  to 20 cm intervals were collected from the natural site to a depth of 109 cm. All soils were air-dried, homogenized and split with a riffle splitter, to produce representative subsamples for subsequent analyses. An assortment of nine solid fertilizers and amendments applied for soil and foliar application were collected from the pecan orchard in 2018, dissolved in de-ionized water and analyzed for major ions as described in detail in following sections (Appendix Table 1A). Gypsum, elemental sulfur pellets and all other fertilizers or

amendments that were not available and thus, not analyzed.

#### 2.3. Soil analyses

# 2.3.1. Soil texture

The bulk soil sample was ground gently with a mortar and pestle to break aggregates and all particles were less than 2 mm. Soil samples were split to three different particle size fractions including sand (0.063–2 mm), silt (0.002 –0.063 mm), and clay (<0.002 mm) using a wet sieving and centrifuge procedure (Jackson, 1967). Specifically, the sand fraction was separated from silt and clay by wet sieving (0.063 mm, Mesh # 230). All finer particles in a slurry were then centrifuged at 3500 rpm for ten minutes. The supernatant contained the clay fraction and was separated from the pellet at the bottom of the centrifuge tube, the silt fraction. All three fractions (sand, silt, and clay) were air dried and then weighed to determine soil texture.

#### 2.3.2. Sequential extraction

The sequential extraction of water-soluble and acid-leachable fractions was conducted for the dust samples and soils from the Pecan\_Coarse, Pecan\_Fine, natural site and Alfalfa\_Fine\_D sites. The amendments and fertilizers used in the pecan orchard and soils from Alfalfa\_Fine and Alfalfa\_Coarse were only characterized for the water-soluble fraction.

#### 2.3.3. Water-soluble fraction:

De-ionized water was used to extract water-soluble salts, such as CaCl<sub>2</sub>, NaCl, CaSO<sub>4</sub>\*2H<sub>2</sub>O or Na<sub>2</sub>SO<sub>4</sub> from the samples (Cox et al., 2018). The resulting water-soluble fraction is directly linked to irrigation and evaluates the evaporite salt buildup, as well as soil salinity and sodicity. For the water-soluble extraction, 10 g of a soil sample was weighed into a centrifuge tube and mixed with 30 mL of de-ionized water (18.2 M $\Omega$ , DI). The 1:3 slurry was shaken for 15 min on a shaker and centrifuged at 3500 rpm for ten minutes. The supernatant was passed through a 0.45  $\mu m$  paper filter and weighed. The leachate was analyzed for electrical conductivity (EC) and pH. The sympHony VWR EC and pH electrodes were calibrated using 1413  $\mu S$  cm $^{-1}$  and 12.9 mS cm $^{-1}$  standards, and pH 4 and pH 7 buffer solutions, respectively. Before elemental analyses, the leachate was diluted to 1:100 with deionized water. Aliquots used for cation concentrations were acidified

with 3–4 drops of ultra-pure  $\rm HNO_3$  and analyzed in a Perkin Elmer 5300DV inductively coupled plasma-optical emission spectrometer (ICP-OES). Aliquots for anion concentrations remained un-acidified and analyzed with a Dionex ICS-2100 ion chromatography (IC) system. A procedure blank was included along with soil and dust samples.

#### 2.3.4. Exchangeable fraction:

The exchangeable cations were removed from the residual soil pellets after the water extraction and before the following acid extraction following the method of Amacher et al. (1990) and White et al. (2005). Specifically, the soil residues, resultant from the water-soluble extraction, were mixed with 25 mL of 0.1 M BaCl<sub>2</sub>-0.1 M NH<sub>4</sub>Cl, shaken for 15 min and then centrifuged at 3500 rpm for five minutes. Residue soils were separated from supernatants, rinsed with 5 mL of DI water and centrifuged for 5 min at 3500 rpm. The data on the exchangeable fraction are not discussed in this paper. The soil residues were used for the subsequent extraction.

#### 2.3.5. Acid leachable extraction:

An acid leachable extraction was used to dissolve carbonate minerals, i.e., pedogenic calcite in this study following the method of Jacobson et al. (2003) and Jin et al. (2010). Specifically, exactly 20 mL of dilute acetic acid were added onto soil residue from the exchangeable fraction (1 M or 2 M depending on calcite contents as estimated from the soil inorganic carbon concentration). The mixture was shaken for six hours and centrifuged at 2500 rpm for 20 min and the supernatant filtered with a 0.45  $\mu$ m paper filter. The soil residue was washed again with 3 mL of 1 M or 2 M acetic acid. Two aliquots of acetic acid leachates were combined, dried and re-dissolved in 2% HNO3, before analysis of cation concentrations on the ICP-OES.

#### 2.3.6. Saturation paste extraction

The Pecan\_BG profiles was sampled previously as Pecan1 and analyzed for its pH, electrical conductivity (ECe) and elemental composition in saturated paste extract (SPE) (Cox et al., 2018). To be consistent and comparable, Pecan\_AG soils were characterized using the same procedure as Rhoades (1996) and Cox et al. (2018).

#### 2.4. Water sample collection and characterization

Four types of water samples were collected only from the pecan orchard: irrigation waters, soil waters, shallow groundwaters, and drainage waters. Irrigation waters were collected prior to each flooding event from irrigation canals (IRW\_RG) or from the local and deep groundwater wells (IRW\_GW). Soil waters were collected typically one week after irrigation, using 1900-series tension lysimeters (Soil Moisture®, Santa Barbara, CA) installed at four depths, 15, 30, 60 and 120 cm respectively. A vacuum of -50 centibar was pulled on the lysimeters one day before irrigation. Drainage waters were also collected seven days after irrigation from the drainage canals. Three wells were installed near Pecan\_Coarse in 2018 to sample shallow groundwaters (Sosa, 2019), and these wells were advanced to depths of 3.5 m (GW1), 2.8 m (GW2), and 2.2 m (GW3) respectively. Samples were collected approximately one week after an irrigation event. At least three well volumes were purged to allow the collection of a representative sample.

The pH and EC of water samples were measured in the field using calibrated probes. The irrigation water, groundwater and drainage water samples were filtered in the field using 0.45  $\mu$ m filters and analyzed for alkalinity and concentrations of major ions. The ceramic cups in the lysimeters have maximum pore size of 1.3  $\mu$ m, so soil water samples were not further filtered. Samples were refrigerated at 4 °C before analysis. Samples for cation analysis were acidified using several drops of ultrapure nitric acid ( $\sim$ 15 N). Water alkalinities were titrated with dilute hydrochloric acid and calculated using the Gran-alkalinity method with the DL15 Mettler-Toledo titrator (Stumm and Morgan, 1996; Drever, 1997). Major cations were analyzed by the ICP-OES and

major anions by the IC.

Procedure blanks and sample replicates were included for QA/QC. The USGS Reference Materials M182 and M178 (water standards) were run as checks on ICP-OES and an in-house water standard for IC. Errors were within 10% of certified values for all major cation concentrations on ICP-OES and 5% for all anion concentrations on IC. The data quality of the leachates in water-soluble fractions were also evaluated by charge balance where concentrations of major cations and anions and alkalinity are measured, as well as regressions between electrical conductivity and the sum of cation charges or sum of anion charges (Appendix Fig. 1).

Saturation indices (SI) for calcite, gypsum and halite were calculated from pH, elemental chemistry using Visual MINTEQ ver 3.1, assuming 20  $^{\circ}$ C as the water temperature. This was to calculate the ratio of ion activity product (IAP) to solubility product in a log unit for a given mineral and a given water sample:

$$SI = log_{10}(\frac{IAP}{K_{vo}}) \tag{1}$$

where water samples are considered at equilibrium with a mineral if the SI equals zero, under-saturated if the SI is negative and supersaturated if the SI is positive. For groundwater samples (GW1, GW2, GW3), alkalinity was not titrated. It was estimated from the difference in the total positive charge of major cations and negative charge of all other anions.

#### 2.5. Soil sensor network

A soil sensor network had been previously established in both the Pecan\_Fine and the Alfalfa\_Fine sites by Cox et al. (2018), where soil volumetric water content (VWC), soil temperature ( $T_{soil}$ ) and bulk soil EC were recorded at depths of 15, 30, 60, and 120 cm with 5TE Decagon sensors and Campbell CR1000 data loggers. For this study, a soil sensor network was established for Pecan\_Coarse soils to compare with Pecan\_Fine site. Previously, a continuous dataset of five-minute resolution was collected from the Pecan\_Fine network for two growing seasons in 2014 and 2015 and for one growing season during 2016. Only one irrigation event was captured for both Pecan\_Fine and Pecan\_Coarse at 15 cm soils during 2016.

Pore-fluid chemistry change in response to evaporation, dissolution and precipitation of secondary salts can be better understood by calculating the real-time variation in pore-fluid EC, with bulk EC from the 5TE sensors (Hillhorst, 2000):

$$\sigma_p = \frac{\dot{\varepsilon_p} * \sigma_b}{\dot{\varepsilon_b} - \dot{\varepsilon_{ab=0}}} \tag{2}$$

where,  $\sigma_p$  is the pore-fluid EC (dS m<sup>-1</sup>);  $\varepsilon_p$  is the unitless real portion of the dielectric permittivity of the soil pore water;  $\sigma_b$  is the bulk EC (dS m<sup>-1</sup>);  $\varepsilon_b$  is the real portion of the bulk soil dielectric permittivity, unitless;  $\varepsilon_{\sigma b=0}$  is the real portion of the dielectric permittivity of the dry soil.  $\varepsilon_p$  can be calculated from the soil temperature by:

$$\varepsilon_p = 80.3 - 0.37*(T_{soil} - 20)$$
 (3)

where  $T_{soil}$  is the soil temperature (°C) and collected from the 5TE sensors. Furthermore,  $\varepsilon_b$  is calculated using the raw volumetric water content (VWC) counts and converting these to bulk dielectric with a calibration:

$$\dot{e_b} = \frac{\varepsilon_{Raw}}{50} \tag{4}$$

 $\dot{e_{ab=0}}$  is an offset term to represent the dielectric permittivity of dry soils and a generic offset of 4.1 is used. Conversion of bulk soil EC to pore-fluid EC through Eq. (2) has been validated by EC measurements on sampled soil waters during the saturated field conditions in this pecan orchard (Cox et al., 2018).

#### 3. Results

#### 3.1. Soil texture

The particle size distribution (PSD) changed dramatically with depth at each soil profile and among different soil profiles (Appendix Table 2; Fig. 2). Indeed, PSD showed strong contrasts between the two soil profiles at the pecan site and between the two soil profiles at the alfalfa site (Fig. 2A-D). The Pecan\_Fine soils were loamy at shallow depths, contained up to 75 wt% clay and almost no sand between 50 cm and 160 cm, and became sandy below the clayey layer (Fig. 2A). Similarly, a finegrained layer was observed at the same depth range of the Pecan\_Coarse soil profile, but with much lower clay content and higher sand content (Fig. 2B). Below 40 cm, more than 50% of sand was observed at Pecan\_Coarse. A Wilcoxon-Rank test showed that Pecan\_Fine soils had significantly higher clay contents than Pecan\_Coarse soils (p < 0.005). Shallow soils from Alfalfa Coarse contained ~ 50% sands, with a

**Fig. 2.** Soil texture for five soil profiles: Pecan\_Fine (A), Pecan\_Coarse (B), Alfalfa\_Fine (C), Alfalfa\_Coarse (D), and the natural site at Fabens (F). Shaded areas illustrate where salt accumulation peaked right above the fine-grained layer.

E. Natural soil

distinctive clay peak between 50 and 140 cm depths followed by sandy soils below (Fig. 2D). The soils from the Alfalfa\_Fine site were dominated by finer silt and clay particles throughout the profile, with a sand% decreasing with depth (Fig. 2C). At the natural Fabens site, soils from the top 10 cm contained almost 90% sand and became finer towards deeper soils. As sand contents gradually decreased, silt contents increased with depth (Fig. 2E).

#### 3.2. Soil sequential extraction

#### 3.2.1. Water-soluble extraction

Chemical compositions of water extraction from eight soil fertilizers and amendments were reported in Appendix Table 1B. These are very soluble and have high concentrations of Ca<sup>2+</sup>, Na<sup>+</sup>, K<sup>+</sup> etc.

The pH, EC and major ion concentrations in the water-soluble fraction of all soils, and dust are reported in Appendix Table 2. Except for two outliers, the sum-total of negative charges (anions) were positively correlated to the sum-total of positive charges (cations) in the water-soluble fraction of all samples. Similarly, EC values were also positively correlated to the sum-total positive charges (Appendix Fig. 1A and 1B). The PSD and water-soluble data of alfalfa soils were presented as graphs and compared to geophysical survey in Doser et al. (2019).

All agricultural soils were slightly basic, with pH ranging narrowly from 7.0 to 8.0. In contrast, soil pH in the natural site changed quickly from 6.6 to 8.3 for the top 20 cm and remained near 7.5 the rest of the profile (Fig. 3A). Soil EC varied drastically with depth and among different sites (Fig. 3B). The Alfalfa\_Coarse and the Pecan\_Coarse sites had the lowest and the least variable EC among all soils. The entire Pecan\_Fine soil profile showed consistently higher EC values between 0.96 and 3.68 dS  $\rm m^{-1}$  than Pecan\_Coarse. The soils at the Alfalfa\_Fine site had much lower EC values than the Pecan\_Fine profile but had a peak of 3.86 dS  $\rm m^{-1}$  around 150 to 250 cm depth. Surprisingly, the highest soil EC values were observed in the natural site; EC increased quickly with depth and reached 6.2 dS  $\rm m^{-1}$  at around 90 cm.

Like EC, concentrations of water-soluble  $\mathrm{Na^+}$ ,  $\mathrm{Ca^{2^+}}$ ,  $\mathrm{Cl^-}$  and  $\mathrm{SO_4^{2^-}}$  were systematically higher in the Pecan\_Fine soils than those in the Pecan\_Coarse soils (Fig. 3C-F). Similarly, the soils at the Alfalfa\_Fine profile also had consistently higher water-soluble concentrations than those at the Alfalfa\_Coarse site. Concentrations of  $\mathrm{Na^+}$ ,  $\mathrm{Ca^{2^+}}$  and  $\mathrm{SO_4^{2^-}}$  in the water-soluble fraction at the natural site were the highest among all soil profiles but its  $\mathrm{Cl^-}$  concentrations were similar as those in the alfalfa and pecan soils.

The dominant cations in the water-soluble fraction were Na<sup>+</sup> and Ca<sup>2+</sup>, followed by Mg<sup>2+</sup> and K<sup>+</sup>, and dominant anions SO<sub>4</sub><sup>2-</sup> and Cl<sup>-</sup> (Appendix Table 2; Fig. 3A). Moreover, the Piper-Hill diagram revealed the soils in the Pecan\_Coarse site have higher water-soluble Na<sup>+</sup> plus K<sup>+</sup> and lower Ca<sup>2+</sup> and Mg<sup>2+</sup> than those in the Pecan\_Fine site (Fig. 4A). Soil SAR values were calculated from water leachates and were below the sodicity threshold of 13 (Fig. 3G). However, this procedure used higher water: soil ratios than typically used in soil salinity and sodicity studies (Cox et al., 2018); hence, SAR, was underestimated. Therefore, it is reasonable to assume most soils from the pecan and alfalfa sites were sodic or close to sodicity. At pecan soils, SAR values were lowered by an average of 60% after gypsum treatments (Fig. 5). Generally, coarser textured soil profiles, Pecan Coarse or Alfalfa Coarse, had lower SAR values than their fine-textured counterparts, Pecan Fine and Alfalfa -Fine. The SAR values for the top 40 cm of the natural site were much lower than those of any agricultural site, but quickly surpassed the sodicity threshold below 40 cm (Fig. 3G).

### 3.2.2. Acid leachable

The predominant cation in the acid leachable extraction was  $\text{Ca}^{2+}$ , with little addition of  $\text{Mg}^{2+}$  (Appendix Table 2; Fig. 6A). Overall, the Pecan\_Fine profile had much higher  $\text{Ca}^{2+}$  than the Pecan\_Coarse profile, with Mg/Ca ratios of 0.04 and 0.03 respectively, indicative of low-Mg calcite. Calcite contents were calculated from the acid leachable  $\text{Ca}^{2+}$ 

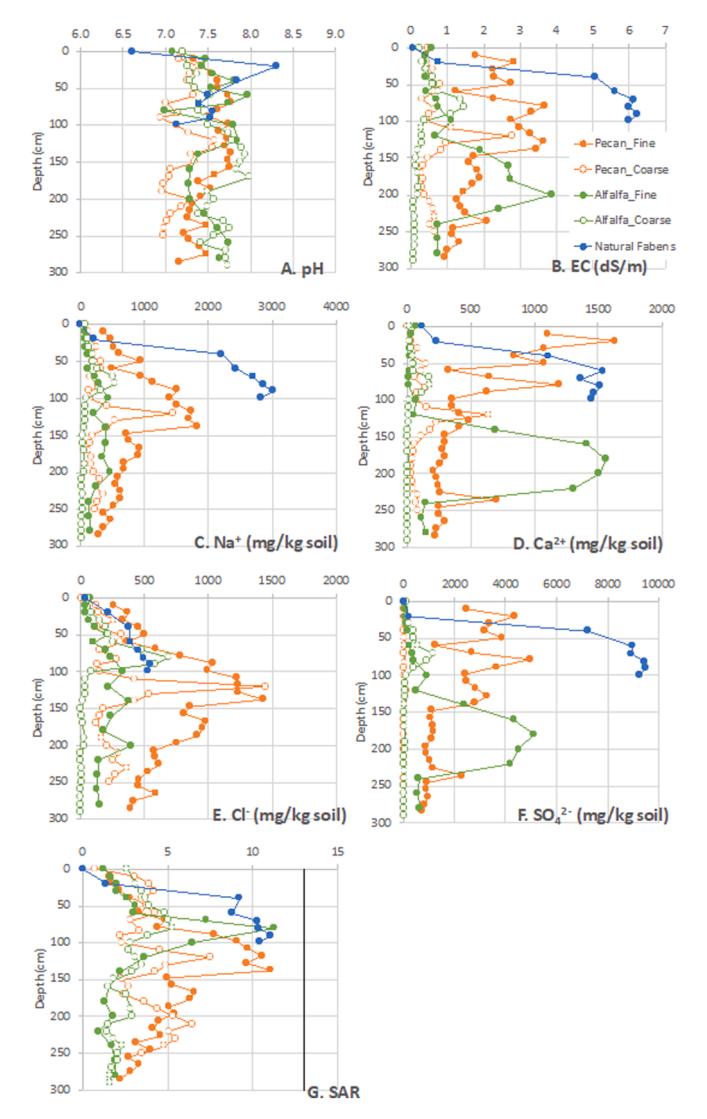


**Fig. 3.** Depth profiles of pH (A), EC (B),  $Na^+$  concentration (C),  $Ca^{2+}$  concentration (D),  $Cl^-$  concentration (E),  $SO_4^{2-}$  concentration (F), and sodium adsorption ratios (SAR, G), in the water-soluble fraction of soils from the pecan, alfalfa and natural Fabens sites.

concentrations assuming CaCO $_3$  stoichiometry. Soils from the Pecan–Fine site contained up to 8 wt% of calcite and those from the Pecan–Coarse site had close to 3 wt% of calcite (Fig. 6B). Soils from Alfalfa\_Fine and Alfalfa\_Coarse profiles were not characterized for acid leachable fraction. However, Alfalfa\_Fine\_D soils had more pedogenic carbonate that the pecan soils (Fig. 6B; Appendix Table 2), averaging 13 wt% CaCO $_3$ . Pedogenic carbonate contents at the natural soils were like those at the Pecan\_Fine site, at  $\sim$  8 and 6 wt% respectively. The acid leachable extraction of the two dust samples from the natural site and the pecan orchard were 3.5 and 3.4 g/kg Ca<sup>2+</sup>, respectively (Appendix Table 2).

# 3.3. Water chemistry

Water chemistry data were reported for the pecan sites in Appendix Table 3 and Fig. 7. Charge balance for the water chemistry was calculated for samples with complete major cation and anion characterization and reported in Appendix Fig. 1C and 1D. Irrigation water samples at the Pecan site were alkaline with pH ranging from 7.3 to 8.8 (Fig. 7A). Soil water pH decreased at 60 cm depths for Pecan\_Fine soils. The groundwater irrigation samples (IRW\_GW) had similar pH values to Rio Grande irrigation waters (IRW\_RG). Alkalinity, EC and major ions (Ca<sup>2+</sup>, Na<sup>+</sup>,

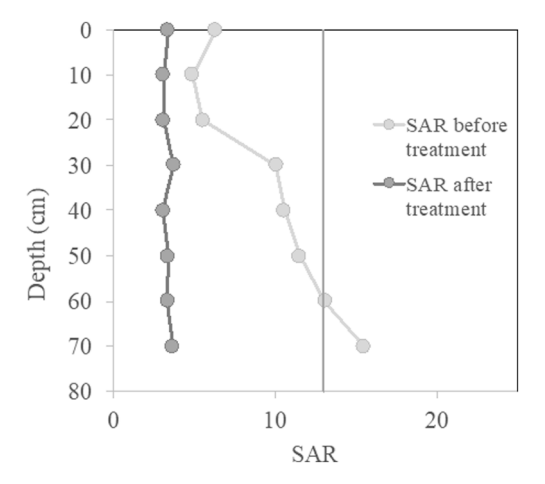


**Fig. 5.** Sodium adsorption ratios (SAR) of soils at the Pecan\_Fine site before and after treatment with gypsum. The threshold for sodic soil is 13, plotted as a vertical line for reference. SAR data before treatment was from Cox et al. (2018). SAR data after treatment were collected using the same method as Cox et al. (2018).

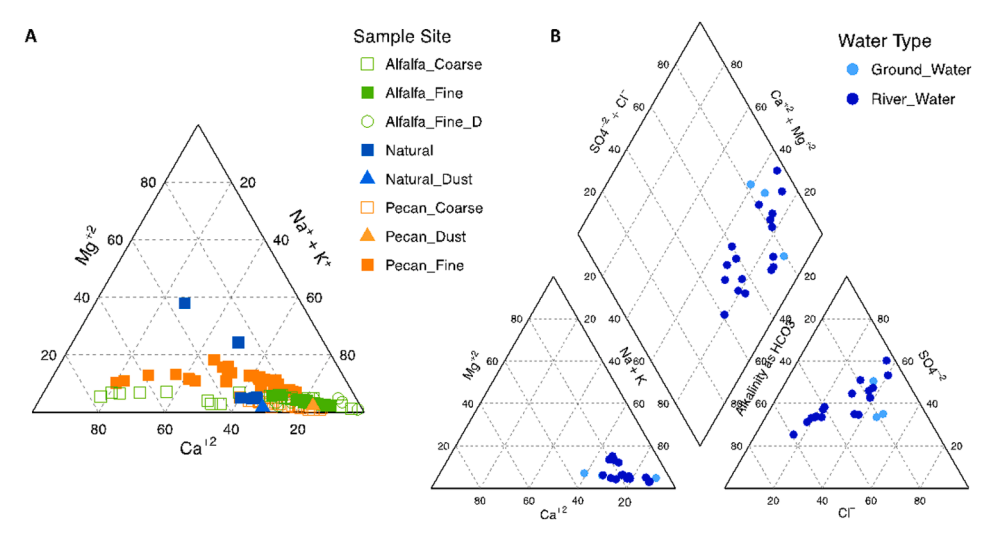
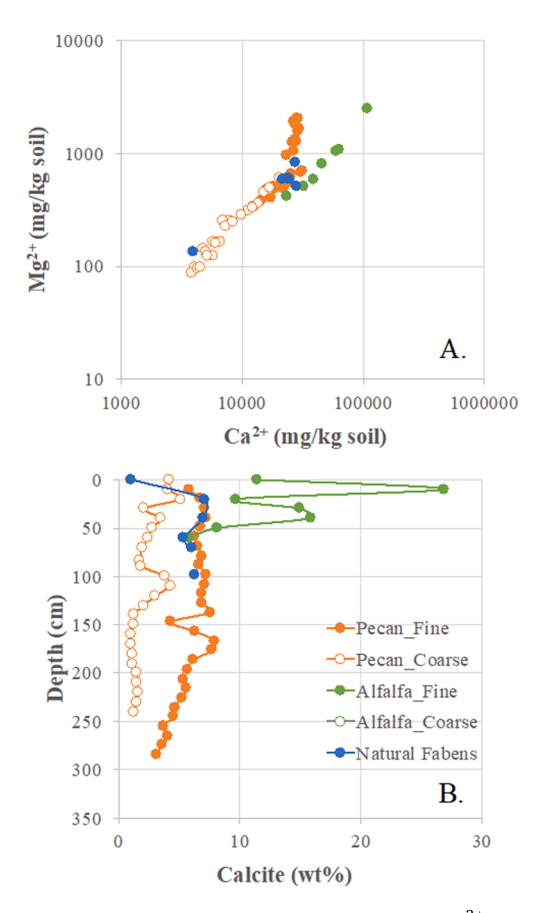


Fig. 4. Piper-Hill diagrams for (A) water leachates of the soils and dust and (B) for irrigation waters (river and deep groundwater).



**Fig. 6.** Acid leachable fraction of all soils is dominated by  ${\rm Mg}^{2+}$  and  ${\rm Ca}^{2+}$  (A), indicating presence of low-Mg calcite. The calcite weight% is plotted as a function of depth (B). Notice that data plotted as Alfalfa\_Fine are collected from Alfalfa\_Fine\_D, a duplicate soil core near Alfalfa\_Fine.

 $\mbox{Cl}^-$  and  $\mbox{SO}_4^{2-}$ ) increased with soil profile depth; however, canal drainage waters (DRW) and shallow groundwaters (GW1-GW3) were similar to irrigation water EC and alkalinity (Fig. 7B-7E).

A Piper-Hill diagram for pecan waters showed that both types of irrigation waters had higher Na $^+$  and K $^+$  concentrations than Ca $^{2+}$  and Mg $^{2+}$  concentrations (Fig. 4B). Irrigation waters from the river (IRW\_RG) tended to have higher alkalinity and  $SO_4^{2-}$  and lower Cl $^-$  than from the deep ground waters (IRW\_GW) (Fig. 7C).

Geochemical modelling indicated that SI values for gypsum were negative  $\sim -2$  and increased with soil depth to reach 0, suggesting that soil waters were under-saturated or near saturation. In contrast, irrigation waters, soil waters and groundwaters were near saturation or oversaturated with respect to calcite, with SI values from 0.06 to 1.4 (Fig. 7F). All water samples were under-saturated with respect to halite, with SI values less than -5.

# 3.4. Soil sensor network

Soil moisture, temperature, bulk EC and calculated pore-fluid EC data at 15 cm depth were plotted for the Pecan\_Fine and Pecan\_Coarse sites, for one irrigation event in 2016 (Fig. 8). The VWC at 15 cm was higher in Pecan\_Fine soils than Pecan\_Coarse soils (Fig. 8A). Soil moisture plateaued at 15 cm while soils were saturated with ponded water, VWC was 0.45 and 0.32  $\rm m^3~m^{-3}$  for Pecan\_Fine and Pecan\_Coarse, respectively. This indicated higher soil porosity at 15 cm at the Pecan\_Fine site than the Pecan\_Coarse site. Differences in the soil moisture were significant between two sites (Wilcoxon Signed-Rank test p-value < 2.2e-16); VWC for both soils returned to pre-flooding values approximately 10 days after irrigation (Fig. 8A). Although flooding led

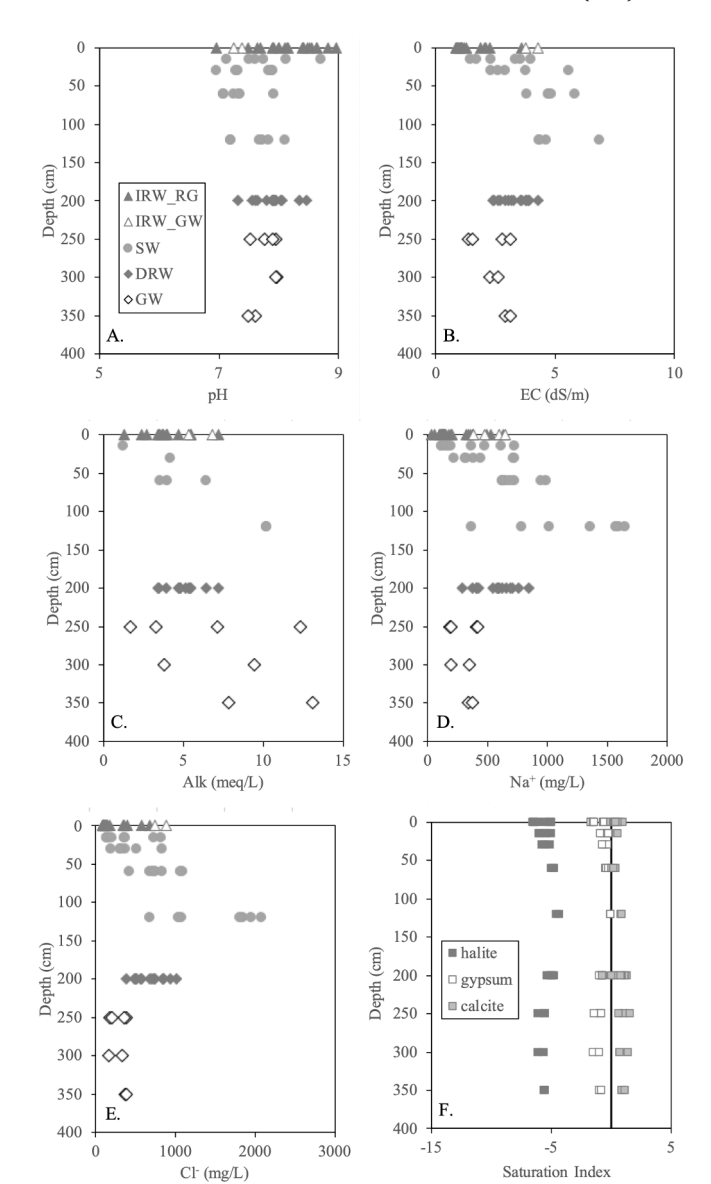


**Fig. 7.** Major element chemistry of all water samples: pH (A), EC (B), alkalinity (C), Na<sup>+</sup> concentrations (D), Cl<sup>-</sup> concentrations (E), and saturation indexes (SI) for halite, gypsum and calcite (F). The irrigation water (IRW) is placed at 0 cm, soil water (SW) is from 15 cm, 30 cm, 60 cm and 120 cm, drainage water (DRW) is placed arbitrarily at 200 cm, and groundwater is placed at 250 cm for GW1, 300 cm for GW2, and 350 cm for GW3. IRW\_RG and IRW\_GW are irrigation waters from Rio Grande and groundwater, respectively.

to lower soil temperatures in coarser textures, both coarse and fine textures followed diurnal patterns, soil temperatures did not return to pre-flooding values (Fig. 8B). Bulk EC was higher at Pecan\_Fine than Pecan\_Coarse (Fig. 8C) and peaked at the onset of irrigation in both soils, then gradually decreased to pre-flooding values. Pore-fluid EC decreased immediately after irrigation in both soils. After a short period of equilibrium of 2 days in fine-textured soils and  $\sim$ 6 h for coarse-textured soils, pore-fluid EC increased slowly, until reaching pre-flooding baseline values. Pecan\_Coarse soils reached baseline values much faster ( $\sim$ 1 day) than Pecan Fine ( $\sim$ 10 days) (Fig. 8D).

#### 4. Discussion

#### 4.1. Salt-loading at the agricultural and natural soils

In this study, salt accumulation can occur from irrigation, rainfall,

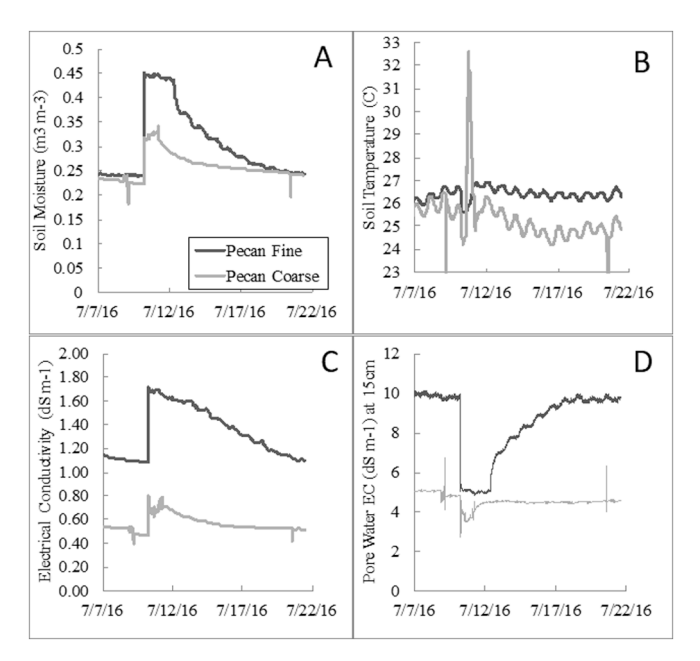


**Fig. 8.** Evolution of soil moisture (volumetric water content, VWC, A), soil temperature (B), bulk soil EC (C) and pore-fluid EC (D) at 15 cm soil depths at the Pecan\_Fine and Pecan\_Coarse site for a flood irrigation event on the whole pecan orchard. Pore-fluid EC was calculated from bulk soil EC and other soil parameters using Eqs. (2)–(4) as discussed in the text.

water-soluble fraction of dust, and water-soluble fraction of fertilizers and soil amendments. Potential salt-loading from Rio Grande irrigation water (~1.12 m of water per growing season) in the El Paso region is substantial for all major species reported: 306 g Na $^+$  m $^-$  yr $^-$ 1, 129 g Ca $^2$ + m $^-$ 2 yr $^-$ 1, 361 g Cl $^-$  m $^-$ 2 yr $^-$ 1, 419 g SO $_4^2$  m $^-$ 2 yr $^-$ 1, and 284 g HCO $_3^-$  m $^-$ 2 yr $^-$ 1 (Appendix Table 14), similar to estimates from Cox et al. (2018). Groundwaters (IRW\_GW) on average had higher EC values (4.02 dS m $^-$ 1, n = 2) than Rio Grande river (IRW\_RG) (2.18 dS m $^-$ 1, n = 12) (Appendix Table 3; Fig. 7); therefore, groundwater has the potential to double the salt-loading rates of Ca $^2$ +, SO $_4^2$ -, Na $^+$ , and Cl $^-$  if it were the sole source of irrigation water (Appendix Table 4).

The National Atmospheric Deposition Program (NADP) National Trends Network (NTN) provides long-term records of elemental loading from precipitation (<a href="http://nadp.slh.wisc.edu">http://nadp.slh.wisc.edu</a>). The annual Ca deposition at five sites that are closest to this study area, each with more than 20 years of record, ranges from 0.08 to 0.24 g Ca $^{2+}$  m $^{-2}$  yr $^{-1}$  and averages at 0.18 g Ca $^{2+}$  m $^{-2}$  yr $^{-1}$  (AZ98: Chiricahua, AZ; NM08: Mayhill, NM; TX2: Muleshoe National Wildlife Refuge, TX; TX16: Sonora, TX; TX22: Guadalupe Mountains National Park Frijole Ranger Station, TX), representing regional loading averages, that are similar to measured values in this study.

The solid fertilizers that were analyzed for this study were extremely water-soluble and would dissolve quickly by irrigation waters once applied at the soil surface. However, the salt loading in the agricultural soils was negligible due to low application rates (Appendix Table 1; Appendix Table 4). A full suite of liquid and solid fertilizers used in the field is needed to quantify the total loadings. However, the soil amendments analyzed contributed significant amounts of dissolved calcium and sulfate (29–58 g  $Ca^{2+}$  m<sup>-2</sup> yr<sup>-1</sup>, 240–310 g  $SO_4^{2-}$  m<sup>-2</sup> yr<sup>-1</sup>), slightly lower than those from the irrigation water (Appendix Table 4).

Of the year-long dust collected for this study, a total of 40 and 59 g  $\,m^{-2}\,\,yr^{-1}$  of dust were loaded to soils at the natural site and the pecan orchard, respectively in 2016. Only 0.3% and 0.2% of the dust was water-soluble Ca $^{2+}$  but 3% and 2% were acid soluble Ca $^{2+}$  at the natural site and pecan orchard, respectively. Dissolved Ca $^{2+}$  was the major ion in both water-soluble and acid leachable dust fractions, consistent with previous studies where dusts have been regarded as a major source of Ca

in pedogenic carbonate of natural dryland soils (McFadden and Tinsley, 1985; Reheis and Hihl, 1995; Whipkey et al., 2000). While soluble  ${\rm Ca^{2+}}$  deposition rates from dust are higher than from the analyzed soil fertilizer deposition (0.1–0.2 g m $^{-2}$  yr $^{-1}$  versus an average of 1.22 g m $^{-2}$  yr $^{-1}$ ) and at similar levels as rain, they are much lower than salt deposition from irrigation water (129–356 g m $^{-2}$  yr $^{-1}$ ; Appendix Table 4). These findings agree with previous works that have recognized dust as an important source of salts in natural desert environments (Monger and Gallegos, 2000; Gile et al., 1981; Capo and Chadwick, 1999; Reheis, 2006; Reheis and Urban, 2011; Floyd and Gill, 2011; White et al., 2015); however, the impact of irrigation overshadows the significance of dust in salt loading.

Continuous irrigation affected soil quality in both the pecan and alfalfa sites, similar to what has been observed in other irrigated arid soils (Falasca et al., 2014; Assouline et al, 2015; Cox et al., 2018). Saturation paste salinities averaged from the entire soil profiles showed EC  $\sim 2.11\,$  $dS m^{-1}$ , 0.64  $dS m^{-1}$ , 1.18,  $dS m^{-1}$  0.37  $dS m^{-1}$ , 0.63  $dS m^{-1}$ , and 4.49 dS m<sup>-1</sup> for Pecan\_Fine, Pecan\_Coarse, Alfalfa\_Fine, Alfalfa\_Coarse, Alfalfa Fine D, and the natural Fabens sites, respectively. In the Pecan Fine and Alfalfa Fine soils, these values were close to the salt tolerance levels of pecan and alfalfa, 2.6 and 2.0 dS m<sup>-1</sup>, respectively (Fig. 3B) (Mass and Grattan, 1999; Picchioni et al., 2000). Although these are values taken from only one point in time, they highlight cumulative salt loads from the previous irrigation events. These values also serve as evidence that fine textured control the depth of salt accumulation and provide valuable insight on the effects of continuous irrigation. Although averaged salinities across these profiles are mostly lower than crop threshold tolerances, the negative effects of their salinities is evidenced in aerial photographs showing stunted crop growth (Fig. 1).

The major source of salinity in the natural Fabens site remains elusive. Calculations using the NADP data, assuming a particle density of  $2000 \text{ kg m}^{-3}$  in 100 cm of soil, an average of  $\sim 1100 \text{ mg}$  Ca  $\text{kg}^{-1}$  soil and 340 mg Na  $\text{kg}^{-1}$  soil could be deposited in 12,000 years from wet deposition. This Ca loading rate is comparable to the measured concentrations in the soil profile, suggesting that atmospheric deposition is the major soluble Ca source, similar to other regional studies (e.g., Capo and Chadwick, 1999). However, a major contributor for Na<sup>+</sup> still remains unknown as the loading rates through rainfall and dust are much lower than those measured concentrations in the soil profile (Appendix Table 2; Fig. 1).

#### 4.2. Physical and chemical controls on salt buildup

As discussed above, the soils within the pecan orchard are still not considered saline or sodic but are approaching the threshold levels after 90 years of soil cultivation (Fig. 3). Therefore, it is critical to understand what controls salt accumulation rates in irrigated systems in order to assess how soil quality responds to continuous irrigation and future climate changes.

# 4.2.1. Soil texture control

Soils used for cultivation along the Rio Grande valley developed on fluvial sediments with variable layers of particle sizes due to antecedent flooding and river meanderings (Hall and Peterson, 2013; Doser et al., 2007, 2019). This heterogeneity in soil texture occurs both vertically and laterally, as observed in two soil profiles, which are less than 50 m apart, at the pecan orchard and the alfalfa field (Figs. 1 and 2). Soils from Pecan\_Fine, Pecan\_Coarse and Alfalfa\_Coarse sites are characterized by finer texture at shallow depths, underlain by coarser and sandy texture; in contrast, soils at the Alfalfa\_Fine and the natural site are relatively coarser at the surface and become much finer at depth (Fig. 2). Within the pecan orchard, both Pecan\_Fine and Pecan\_Coarse sites have a layer of finer particles between 100 and 150 cm; however, this layer is silty-clay at the Pecan\_Fine but is still sandy at the Pecan\_Coarse (Fig. 2A, 2B).

Soil texture heterogeneity exerts a strong control on location and rates of salt accumulation in irrigated soils, similar to what others have observed (Eshel et al., 2003; Ganjegunte et al., 2012; Cox et al., 2018). The absolute EC values measured from the soil leachates are sensitive to the soil: water mixing ratio in the slurry, the same ratio was used for all soil samples in this study; therefore, EC values are comparable among different sites as a proxy of total salt buildup (Appendix Table 2). Both Pecan\_Coarse and Alfalfa\_Coarse soils had average profile EC values 3X lower than their fine soil counterparts, the Pecan Coarse soils, had lower EC than Pecan Fine soils; similarly, Alfalfa Coarse soils had lower EC values than Alfalfa\_Fine soils (Fig. 3B). Within each soil profile, the EC peak was typically observed around the finer-textured soil layers (shaded areas in Fig. 2, Appendix Fig. 2). For both pecan sites, the highest EC values are between 100 and 150 cm; at the alfalfa field, EC peaks are between 150 and 250 cm and between 50 and 100 cm for the Alfalfa\_Fine and Alfalfa\_Coarse profiles, respectively (Fig. 2). This clearly suggests that finer soils limit the water infiltration and lead to more soil buildup.

Salt buildup in agricultural soils is the result of the mass balance between salt input and output fluxes. From the sources collected and analyzed in this study, this work identifies the predominant inputs as irrigation, followed by soil amendments, with minimal additions from atmospheric inputs or soil fertilizers. The outputs are sensitive to soil texture, soil permeability, and consequent salt leaching. Indeed, the 15 cm Pecan\_Fine soil has the twice soil moisture content as the 15 cm Pecan\_Coarse soil following flood irrigation (Fig. 8A). Soil moisture content decreased to the same baseline level after  $\sim$  14 days in both pecan soils. Since water loss through transpiration and infiltration is expected to be slower in the Pecan\_Fine site due to finer soil texture and the small-sized pecan trees up taking water and the soils' higher temperature, it is reasonable to conclude evaporation is higher at Pecan\_Fine than Pecan\_Coarse. If so, it should impact pore-water chemistry as discussed below.

Bulk soil EC increased dramatically at the onset of irrigation, stressing how VWC controls bulk EC (Fig. 8C). Conversion of bulk soil EC to pore-fluid EC highlights soil water chemistry and its evolution across evaporation and chemical reactions. As shown in Fig. 8D, soil water EC, similar to irrigation EC, was low at the onset of flood irrigation and undersaturated with respect to gypsum and halite, SI < 0 (Fig. 7). After the irrigation event, pore-fluid EC increased with the dissolution of previously accumulated evaporate salts. Both soils reached varying equilibrium, dependent on the individual soils' initial EC. Soil texture controlled water equilibrium with existing salts; Pecan\_Fine soil reached equilibrium within two days and Pecan\_Coarse within one day. Evaporation lowered soil moisture contents (Fig. 8A) while increasing pore-fluid EC towards mineral saturation, presumably leading to secondary salt precipitation (Fig. 8D).

Major ion concentrations and EC increased with depth; as a result, SI of both gypsum and halite came closer to saturation in the pecan orchard soil waters (Fig. 7F). As discussed above, the floodplain mud interfingerings limit the depth at which waters leach salts and lower the connectivity of shallow soils and underlying aquifers. Furthermore, increased salt accumulation in these fine-textured layers could also decrease available pore space, lowering hydraulic connectivity and permeability. As impermeable layers restrict water movement, lateral flow towards return and drainage waters is expected during saturated field conditions. With limited water infiltration from above, soil salt contents were much lower below the clayey layers in pecan soils.

#### 4.2.2. Solubility control

Soil waters were only sampled during initial irrigation and an evolution of elemental chemistry from irrigation and soil waters is observed: as irrigation waters infiltrate pecan soils, soil waters evolved dramatically, with higher  $\text{Ca}^{2+}$  and  $\text{SO}_4^{2-}$  concentrations and slightly higher  $\text{Na}^+$  and  $\text{Cl}^-$  concentrations (Fig. 7). This evolution could be a result of dissolution of gypsum and halite salts previously accumulated in those zones or dissolution of soil amendments. Towards the end of an irrigation event, gypsum and minor halite should reprecipitate in soils. In

contrast, irrigation waters and soil waters were oversaturated or near saturation with respect to calcite (Fig. 7F). Therefore, calcite is expected to accumulate throughout the irrigation season, similar to what has been previously expected by Szynkiewicz et al. (2015) and reported in Cox et al. (2018), where up to 8 wt% of calcite was observed in these study sites (Fig. 6B). The Pecan\_Fine soils contained higher calcite than the Pecan\_Coarse soils. Peaks in calcite typically occurred above or coincided with peaks in clay in both pecan soil profiles, where calcite abundance was explained by clay contents (linear regression  $R^2=0.30$  and  $R^2=0.24$  for Pecan\_Coarse and Pecan\_Fine, respectively). Although still unsaturated in soil waters, gypsum and halite can precipitate in soils when intensive evapotranspiration concentrates dissolved  $Na^+$ ,  $Cl^-$ ,  $Ca^{2+}$ , and  $SO_4^{2-}$  (Graham and O'Green, 2010).

Contrasting solubility in secondary salt phases also explained the different composition of water-soluble soil fractions and irrigation water, as observed in Piper-Hill diagrams (Fig. 4). The irrigation water is clustered near Na $^+$  plus K $^+$  for cations; however, the water-soluble fraction in soils has slightly higher contribution from Ca $^{2+}$ . This is due to both the addition of Ca from irrigation waters, soil amendments, and dust but more importantly due to the lower solubility of gypsum than halite. As such, Na $^+$  is more likely to remain in the water and leached out from soils than Ca $^{2+}$ .

# 4.3. Short-term and long-term effects of using soil amendments

Soil amendments are commonly used to mitigate soil sodicity, specifically gypsum and sulfur pellets are used at the pecan orchard after each growing season (Choudhary et al., 2004; Lal, 2007; Ganjegunte et al., 2018; Cox et al., 2018). Gypsum, for example, is applied episodically and only to areas of severe sodicity. The improvement in soil quality was observed in soils collected before and after gypsum was added at the Pecan\_Fine sites: SAR values decrease by 60% after the treatment and well below the sodic threshold (Fig. 5). However, irrigation with water of high Na<sup>+</sup> concentrations during the next growing season will increase the soil SAR values again, suggesting the critical need of annual application of soil amendments to maintain the agricultural functionality.

#### 4.4. Potential impacts on groundwater and Rio Grande water quality

Ninety years of soil cultivation in the Rio Grande region have deteriorated the soil quality and this soil degradation can be expected to worsen in the near future as discussed below. More efficient and effective irrigation methods should be considered as an alternative sustainable practice and may slow the soil salinization process (Thompson et al, 2010; Hanson, 2011). Soil amendments temporarily lower soil sodicity, improve water infiltration and increase salt leaching, this practice, although costly, must continue.

The accumulation of secondary salts including calcite, lower soil porosity and permeability and promote additional salt buildup (Cox et al., 2018). Furthermore, waters used for irrigation, Rio Grande or local groundwater, have high Na $^+$  concentrations relative to Ca $^{2+}$  and Mg $^{2+}$  concentrations, which result in agricultural soils of high salinity and high sodicity (Fig. 4, Fig. 3G). Under these conditions, clay particles remain flocculated; however, if the sodicity-salinity balance is broken, clay disperses, lowering the permeability in fine-texture soils even more.

Increased regional temperatures and reduced snowpack at the headwaters, as well as human activities, are anticipated to impact the quality and quantity of Rio Grande water (Phillips et al., 2003, 2011; Swetnam and Betancourt, 1998; Seager and Vecchi, 2010; Gutzler and Robbins, 2010). Not only is the Rio Grande expected to become more saline as climate change occurs (Borrok and Engle, 2014), but the limited water availability can drive stakeholders to increase their groundwater use for irrigation. A change to a water source of lower quality could increase soil salinization rates, groundwater table depth and regional cones of depression (Sheng, 2013) (Fig. 9). If unchecked or

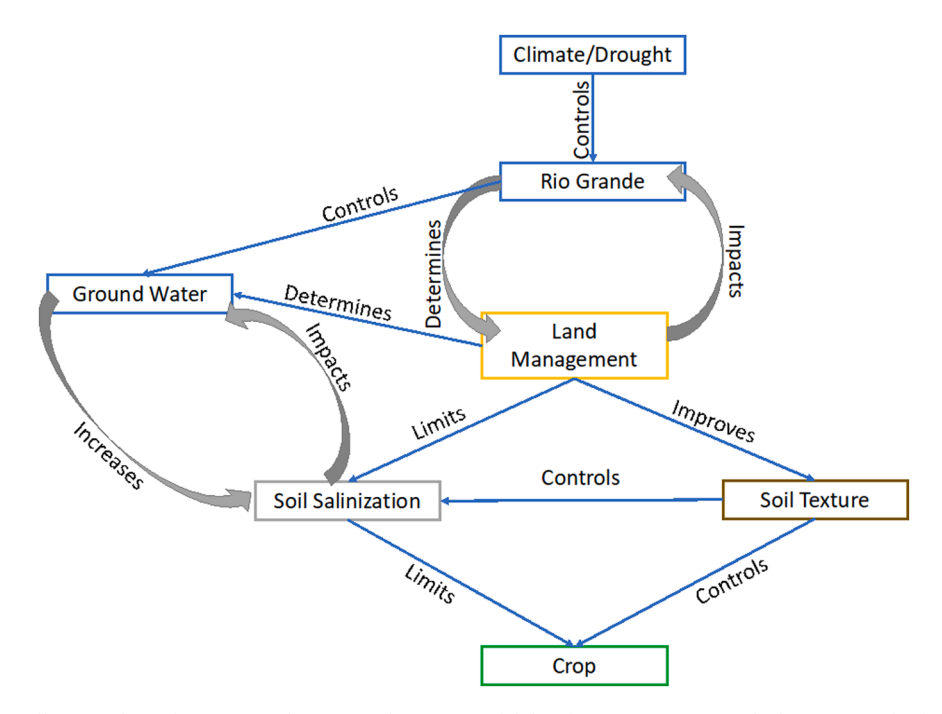


Fig. 9. Conceptual model to illustrates how climate controls Rio Grande water availability for irrigation. Diminished river water leads to increased use of ground waters by stake holders for irrigation which increase soil salinization. Soil salinization could in turn increase groundwater quality. Additionally, land management practices can improve soil texture and limit salinization with soil treatments and amendments, which will impact crop yields.

mitigated, soil salinization can lead to low crop productivity and low economic returns (Hu and Schmidhalter, 2002).

The flushing of salts and other soil amendments to local groundwater through and to the Rio Grande through infiltration and drainage return flow, will greatly impact water quality. Consequently, soil and freshwater sustainability is controlled by agricultural practices and soil management in irrigated drylands, such as in the Rio Grande valley.

# 5. Conclusion

This case study highlights the water-soil interaction in irrigated aridlands, it also highlights and supports current practices and steps taken to combat excessive soil salinization. This study also shows that successful cultivated agriculture requires continuous management to maintain sustainability, functionality and to combat soil salinization, as soils may surpass critical SAR values within one irrigation season. This study found that flood irrigation was the major source of salinization in agricultural soils; and from the collected and analyzed endmembers, assign the salt-loading sources presented here in order of importance as: groundwater irrigation > Rio Grande irrigation > amendments > dust > fertilizers. Increased and continued land-management can limit the amount of salts that accumulate in soils. Soil texture is the major control on water and salt movement, controlling soil water flow paths, residence time, and rates and locations of salt buildup. Although gypsum application and other soil amendments temporarily decrease sodicity, continued irrigation with Na<sup>+</sup>-rich Rio Grande or local groundwaters will again increase soil sodicity. Among all secondary salts, calcite precipitation is the most significant, due to its low solubility, followed by gypsum and halite. Predicted increases in surface water salinity and decreases in availability due to climate changes can lead to increased groundwater use and elevated soil salinization of agricultural soils.

# **Declaration of Competing Interest**

The authors declare that they have no known competing financial interests or personal relationships that could have appeared to influence the work reported in this paper.

#### Acknowledgements

Part of this work was sponsored by the Southwest Consortium for Environmental Research and Policy (SCERP) through a cooperative agreement with the U.S. Environmental Protection Agency (EM-834861-01). Financial support was also from the National Science Foundation under award number 1853680. The owners of the alfalfa and pecan fields, the Ivey family, are greatly acknowledged for their support and collaboration. We thank Alyssa Le Mar, Manny Sosa, and Karen Valles for their assistance in the field and laboratory work. A.C.O. acknowledge summer support from UTEP Dodson graduate fellowship and by the National Institute of Food and Agriculture, U.S. Department of Agriculture, under award number 2015-68007-23130.

# Appendix A. Supplementary data

Supplementary data to this article can be found online at https://doi.org/10.1016/j.geoderma.2021.114976.

### References:

Amacher, M.C., Henderson, R.E., Breithaupt, M.D., Sele, C.L., LaBauve, J.M., 1990. Unbuffered and buffered salt methods for exchangeable cations and effective cation-exchange capacity. Soil Sci. Soc. Am. J. 54, 1036–1042.

Assouline, S., et al., 2015. Balancing water scarcity and quality for sustainable irrigated agriculture. AGU Publications Water Resour. Res. https://doi.org/10.1002/2015WR017071.

Borrok, D.M., Engle, M.A., 2014. The role of climate in increasing salt loads in dryland rivers. J. Arid Environ. 111, 7–13.

Brandy, N.C., Weil, R.R., 2008. The nature and properties of soils, fourteenth ed. Prentice Hall, Pearson.

Capo, R.C., Chadwick, O.A., 1999. Sources of strontium and calcium in desert soil and calcrete. Earth Planet. Sci. Lett. 170 (1), 61–72.

Chaganti, V.N., Crohn, D.M., 2015. Evaluating the relative contribution of physiochemical and biological factors in ameliorating a saline-sodic soil amended with composts and biochar and leached with reclaimed water. Geoderma 259–260, 45–55.

Chavarria, S.B., Gutzler, D.S., 2018. Observed changes in climate and streamflow in the Upper Rio Grande Basin. J. Am. Water Resour. Assoc. 54 (3), 644–659.

Chemura, A., Kutywayo, D., Chagwesha, T.M., Chidoko, P., 2014. An assessment of irrigation water quality and selected soil parameters at Mutema Irrigation Scheme, Zimbabwe. J. Water Resour. Protect. 6, 132–140.

- Chiquet, A., Michard, A., Nahon, D., Hamelin, B., 1999. Atmospheric input vs in situ weathering in the genesis of calcretes: a Sr isotope study at Galvez (Central Spain). Geochim. Cosmochim. Acta 63, 311–323.
- Chiquet, A., Colin, F., Hamelin, B., Michard, A., Nahon, D., 2000. Chemical mass balance of calcrete genesis on the Toledo granite (Spain). Chem. Geol. 170, 19–35.
- Choudhary, O.P., et al., 2004. Effect of sustained sodic and saline-sodic irrigation and application of gypsum and farmyard manure on yield and quality of sugarcane under semi-arid conditions. Field Crops Res. 87, 103–116.
- Cox, C., Jin, L., Ganjegunte, G., Borrok, D., Lougheed, V., and Ma, L., 2018. Changes of soil quality due to flood irrigation in agricultural fields along the Rio Grande in western Texas. Applied Geochemistry 90, 87-100, doi.org/10.1016/j. apgeochem.2017.12.019.
- Crutzen, P.J., 2002. Geology of mankind. Nature 415, 23.
- Doser, D.I., Baker, M.R., Langford, R.P., Imana, E.M.C., 2007. Agricultural soils maps as a framework for conducting shallow subsurface investigations in the Rio Grande Valley near El Paso, Texas. Extended Abstract for the 20<sup>th</sup> EEGS Symposium on the Application of Geophysics to Engineering and Environmental Problems.
- Doser, D.I., Ornelas, M.A., Martinez, I., Jin, L., Ortiz, A.C., Kaip, G.M., 2019. Using geophysics to investigate texture and salinity of agricultural soils and their impact on crop growth in the El Paso county, Texas. J. Environ. Eng. Geophys. 24 (3), 465–477.
- Drever, J.I., 1997. The Geochemistry of Natural Waters: Surface and Groundwater Environments. Upper Saddle River, New Jersey.
- Elias, E., Rango, A., Steele, C.M., et al., 2015. Assessing climate change impacts on water availability of snowmelt-dominated basins of the Upper Rio Grande Basin. J. Hydrol.: Regional Stud. 3, 525–546.
- Eshel, G., Fine, P., Singer, M.J., 2003. Total soil carbon and water quality: an implication for carbon sequestration. Soil Soc. Am. J. 71, 397–405.
- Essington, M.E., 2003. Soil and Water Chemistry an Integrative Approach. CRC Press, Boca Raton, FL.
- Falasca, S.L., Ulberich, A., Acevedo, A., 2014. Identification of Argentinian saline drylands suitable for growing Salicornia bigelovii for bioenergy. Int. J. Hydrogen Energy 39, 8682–8689.
- Floyd, K.W., Gill, T.E., 2011. The association of land cover with aeolian sediment production at Jornada Basin, New Mexico, USA. Aeolian Res. 3 (1), 55–66.
- Ganjegunte, G.K., Clark, J.A., Parajulee, M.N., Enciso, J., Kumar, S., 2018. Salinity Management in Pima Cotton Fields Using Sulfur Burner. Agrosyst. Geosci. Environ. 1–10.
- Ganor, E, 1975. Dust in Israel. Sedimentological and Meteorological Analysis of Dust Deposition. Doctoral Thesis. Hebrew University of Jerusalem.
- Ganjegunte, G.K., Sheng, Z., Clark, J., 2012. Soil salinity and sodicity appraisal by electromagnetic induction in soils irrigated to grow cotton. Land Degrad. Develop. https://doi.org/10.1002/ldr.1162.
- Gile, L.H., 1961. A classification of ca horizons in the soils of a desert region, Dona Ana County, New Mexico. Soil Sci. Soc. Am. Proc. 25, 52–61.
- Gile, L.H., Hawley, J.W., Grossman, R.B., 1981. Soils and geomorphology in the Basin and Range area of Southern New Mexico: Guidebook to the Desert Project. New Mexico Bureau of Mines and Mineral Resources.. Socorro. NM, 222.
- Grace, J., Jośe, J. S., Meir, P., Miranda, H. S., and Montes, R. A.: Productivity and carbon fluxes of tropical savannas, J. Biogeogr., 33, 387–400, doi:10.1111/j.1365-2699.2005.01448.x, 2006.
- Graham, R.C., O'Green, A.T., 2010. Soil mineralogy trends in California landscapes. Geoderma 154, 418–437.
- Gutzler, D.S., Robbins, T.O., 2010. Climate variability and projected change in the western United States: regional downscaling and drought statistics. Climate Dyn. https://doi.org/10.1007/s00382-010-0838-7.
- Hall, S.A., Peterson, J.A., 2013. Floodplain construction of the Rio Grande at El Paso, Texas, USA: response to Holocene climate change. Quatern. Sci. Rev. 65, 102–119.
- Hanson, B., May, D., 2011. Drip irrigation for row crops. University of California, Agriculture and Natural. Resources 8447.
- Hillhorst, M.A., 2000. A pore water conductivity sensor. Soil Sci. Soc. Am. J. 64, 192201925.
- Hogan, J., et al., 2007. Geologic origins of salinization in a semi-arid river: the role of sedimentary basin brines. Geology 35 (12), 1063–1066.
- Hu, Y., Schmidhalter, U., 2002. Limitation of salt stress to plant growth. In: Hock, B., Elstner, C.F. (Eds.), Plant Toxicology. Marcel Dekker Inc., New York, pp. 91–224.
- International Boundary & Water Commission.(n.d.) About the Rio Grande. (https://www.ibwc.gov/CRP/riogrande.htm).
- Jackson, M.L., 1967. Soil Chemical Analysis. Prentice-Hall Inc, Englewood, NJ, p. 498. Jacobson, A.D., Blum, J.D., Chamberlain, C.P., Craw, D., Koons, P.O., 2003. Climatic and tectonic controls on chemical weathering in the New Zealand Southern Alps. Geochim. Cosmochim. Acta 67, 29–46.
- Jin, L., Ravella, R., Ketchum, B., Bierman, P.R., Heaney, P., White, T., Brantley, S.L., 2010. Mineral weathering and elemental transport during hillslope evolution at the Susquehanna/Shale Hills Critical Zone Observatory. Geochim. Cosmochim. Acta 74, 3669–3691.
- Kukal, M.S., Irmak, S., 2019. Irrigation-limited yield gaps: trends and variability in the United States post-1950. Environ. Res. Commun. 1, 061005.
- Lal, R., Hall, G.F., Miller, F.P., 1989. Soil Degradation: I. Basic Processes. Land Degrad. Rehabil. 1, 51–69.
- Lal, R., 2007. Carbon management in agricultural soils. Mitigation and Adaptation Strategies for Global Change 12, 303–322.
- Marschner, H., 1995. Mineral Nutrition of Higher Plants, 2nd ed. Academic Press, London.
- Martinez-Beltran, J., Manzur, C.L., 2005. Overview of salinity problems in the world and FAO strategies to address the problem. Proceedings of the international salinity forum

Mass, E.V., and S.R. Grattan., 1999. Crop yields as affected by salinity. In R.W. Skaggs and J. van Schilfgaarde, eds., Agricultural Drainage. Agron. Monograph 38. ASA, CSSA, SSSA, Madison, WI.

- Mass, E.V., Hoffman, G.J., 1977. Crop salt tolerance-current assessment. J. Irrigation Drainage Division 103, 2.
- McFadden, L.D., Tinsley, J.C., 1985. Rate and depth of pedogenic carbonate accumulation in soils: formation and testing of a compartment model. Geol. Soc. Am. 203, 23–43.
- $\label{eq:miyamoto} \mbox{Miyamoto, S., Riley, T., Gobran, G., Petticrew, J., 1986. Effects of saline water irrigation on soil salinity, pecan tree growth and nut production*. Irrig. Sci. 7, 83–95.}$
- Miyamoto, S., 2010. Salt leaching in pecan orchards of the Southwest. Pecan South
- Monger, H.C., Gallegos, R.A., 2000. Biotic and abiotic processes and rates of pedogenic carbonate accumulation in the southwestern United States—relationship to atmospheric CO<sub>2</sub> sequestration. Global climate change and pedogenic carbonates. CRC, Boca Raton, Fla, pp. 273–289.
- Naiman, Z., Quade, J., Patchett, P.J., 2000. Isotopic evidence for eolian recycling of pedogenic carbonate and variations in carbonate dust sources throughout the southwest United States. Geochim. Cosmochim. Acta 64 (18), 3099–3109.
- Pannell, D., Ewing, M., 2006. Managing secondary dryland salinity: Options and challenges. Agricultural Water Management 80, 41–56.
- Pascolini-Campbell, M., Seager, R., Pinson, A., Cook, B.I., 2017. Coverability of climate and streamflow in the Upper Rio Grande from interannual to interdecadal timescales. J. Hydrol.: Regional Stud. 13, 58–71.
- Phillips, F.M., Emlen, Hall G., Black, M., 2011. Reining in the Rio Grande: People, Land, and Water. University of New Mexico Press.
- Phillips, F.M., Hogan, J., Mills, S., Hendricks, M.H., 2003. Environmental tracers applied to quantify causes of salinity in arid-region rivers: Preliminary results from the Rio Grande, southwestern USA. In: Alsharha, A.S., Wood, W.W. (Eds.), Water resources perspective: evaluation, management, and policy: Developments in water science, V50. Elsevier Science, Amsterdam, pp. 327–334.
- Picchioni, G.A., Karaca, H., Boyse, L.G., McCaslin, B.D., Herrera, E.A., 2000. Salinity, boron, and irrigated pecan productivity along New Mexico's Rio Grande basin. J. Environ. Qual. 29, 955–963.
- Qadir, M., et al., 2014. Economics of salt-induced land degradation and restoration.

  Natural Resour. 38, 282–295.
- Qi, Z., et al., 2018. Spatial distribution and simulation of soil moisture and salinity under mulched drip irrigation combined with tillage in an arid saline irrigation district, northwest China. Agric. Water Manage. 201, 219–231.
- Reheis, M.C., Hihl, R., 1995. Dust deposition in southern Nevada and California, 1984-1989: Relations to climate, sources area, and source lithology. J. Geophys. Res. 100, 8893–8918.
- Reheis, M.C., Urban, F.E., 2011. Regional and climatic controls on seasonal dust deposition in the southwestern US. Aeolian Res. 3 (1), 3–21.
- Reheis, M.C., 2006. A 16-year record of eolian dust in southern Nevada and California, USA: controls on dust generation and accumulation. J. Arid Environ. 67, 487–520.
- Rengasamy, P., Marchuk, A., 2011. Cation ratio of soil structural stability (CROSS). Soil Res. 39, 280–285.
- Reynolds, J.F., Stafford Smith, D.M., Lambin, E.F., Turner, B.L., Mortimore, M., Batterbury, S.P.J., Downing, T.E., Dowlatabadi, H., Fernandez, R.J., Herrick, J.E., Huber-Sannwald, E., Jiang, H., Leemans, R., Lynam, T., Maestre, F.T., Ayarza, M., Walker, B., 2007. Global desertification: building a science for dryland development. Science 316, 847–851.
- Rhoades, J.D., 1996. Salinity: electrical conductivity and total dissolved solids. In: Sparks, D.L. (Ed.), Methods of Soil Analysis. Part 3. Chemical Methods. SSSA Book Ser. 5. Soil Science Society of America, Madison, WI, pp. 417–436.
- Richards, L.A., 1954. Diagnosis and improvement of saline and alkali soils. Science 120 (3124), 800.
- Rozema, J., Flowers, T., 2008. Crops for a salinized world. Science 322, 1478–1481. Seager, R., Vecchi, G.A., 2010. Greenhouse warming and the 21st century hydroclimate
- of southwestern North America. PNAS 107 (50), 21277–21282.
  Shannak, B., Corsmeier, U., Kottmeier, Ch., Al-azab, T., 2014. Wind tunnel study of twelve dust samples by large particle size. Atmospheric Environment 98, 442–453.
- Sheng, Z., 2013. Impacts of groundwater pumping and climate variability on groundwater availability in the Rio Grande Basin. Ecosphere 4 (1), 5. https://doi. org/10.1890/ES12-00270.1.
- Shrivastava, P., Kumar, R., 2015. Soil salinity: a serious environmental issue and plant growth promoting bacteria as one of the tools for its alleviation. Saudi J. Biol. Sci. 22, 123–131.
- Soil Survey Staff, Natural Resources Conservation Service, United States Department of Agriculture. Web Soil Survey. Available online at the following link: http:// websoilsurvey.sc.egov.usda.gov/. Accessed [May/16/2018].
- Sosa, E, 2019. A Quantitative Assessment Of Trace Metals In Subsurface Soils And Groundwater In Agricultural Fields Of El Paso, Texas. Open Access Theses & Dissertation. In preparation.
- Stumm, W., Morgan, J.J., 1996. Aquatic chemistry, third ed. Wiley-Interscience, New York
- Swetnam, T.W., Betancourt, J.L., 1998. Mesoscale disturbance and ecological response to decadal climatic variability in the American Southwest. J. Clim. 11, 3128–3147.
  Stables J. 1000. Solt offsetd cells. CIP. Press Peop Peop Peop
- Szablocs, I., 1989. Salt affected soils. CRC Press, Boca Raton.
- Szynkiewicz, A., et al., 2015. Isotopic studies of the Upper and Middle Rio Grande. Part 2- Salt loads and human impacts in south New Mexico and west Texas. Chem. Geol. 411, 336–350.
- Thompson, T., Roberts, T., Lazarovitch, N., 2010. Managing soil salinity with subsurface drip irrigation. World Congress of Soil Science, Soil Solutions for a Changing World.

- Wang, X., Yang, J., Liu, G., et al., 2015. Impact of irrigation volume and water salinity on winter wheat productivity and soil salinity distribution. Agric. Water Manage. 149, 44–54
- Wang, L., D'Odorico, P., Evans, J.P., Eldridge, D.J., McCabe, M.F., Caylor, K.K., King, E. G., 2012. Dryland ecohydrology and climate change: critical issues and technical advances. Hydrol. Earth. Syst. Sci 16, 2585–2603.
- Whipkey, C.E., Capo, R.C., Chadwick, O.A., Stewart, B.W., 2000. The important of sea spray to the cation budget of a coastal Hawaiian soil: a strontium isotope approach. Chem. Geol. 168, 37–48.
- White, A.F., Schulz, M.S., Vivit, D.V., Blum, A.E., Stonestrom, D.A., Harden, J.W., 2005. Chemical weathering rates of a soil chrono-sequence on granitic alluvium: III.
- Hydrochemical evolution and contemporary solute fluxes and rates. Geochim. Cosmochim. Acta 69, 1975–1996.
- White, W.H., Nicole, P.H., Krystyna, T., Sinan, Y., Randy, S.R., Thomas, E.G., Jin, L., 2015. Regional transport of a chemically distinctive dust: gypsum from White Sands, New Mexico (USA). Aeolian Res. 16, 1–10.
- Williams, A., Crossey, L.J., Karlstrom, K.E., et al., 2013. Hydrogeochemistry of the Middle Rio Grande aquifer system—fluid mixing and salinization of the Rio Grande due to fault inputs. Chem. Geol. 351, 281–298.
- Woodhouse, C.A., Kunkel, K.E., Easterling, D.R., Cook, E.R., 2005. The twentieth-century pluvial in the western United States. Geophys. Res. Lett. 32, 7. https://doi.org/ 10.1029/2005GL022413.